ISSN 1392–1320 MATERIALS SCIENCE (MEDŽIAGOTYRA). Vol. X, No. X. 2023

# Amino-acid Based Ferroelectric Nanocomposites from Glycine Sodium Nitrate and Nanodispersed Silicon Dioxide: Preparation, Structure and Electrophysical Properties

**Bich Dung MAI [1*], Thi Nhan LUU [2], Thi Hoa NGO [2], Hoai Thuong NGUYEN [3]**

[1] *Institute of Biotechnology and Food Technology, Industrial University of Ho Chi Minh City, Nguyen Van Bao 12, 700000, Ho Chi Minh City, Vietnam*
[2] *Faculty of Fundamental Science, Hanoi University of Industry, No. 298, Cau Dien Street, Bac Tu Liem District, Hanoi, Vietnam*
[3] *Faculty of Electrical Engineering Technology, Industrial University of Ho Chi Minh City, Nguyen Van Bao 12, 700000, Ho Chi Minh City, Vietnam*

crossref http://dx.doi.org/10.5755/j02.ms.31215

*Received 21 April 2022; accepted 20 May 2022*

For the first time, the nanocomposites from glycine sodium nitrate (GSN) and nanoparticles of silicon dioxide ($nSiO_2$) have been synthesized using a slow evaporation technique. Observed that the optimal content of $nSiO_2$ was estimated as 16.7 wt.%, any deviation from which affected the growth of GSN crystals in the composite, phase transition temperature, dielectric constant, and characteristics of dielectric hysteresis loops. All the anomalies will be thoroughly explained with the evidence of structural data of X-ray diffraction (XRD) and Fourier-transform infrared spectroscopy (FTIR).

*Keywords:* glycine sodium nitrate, silicon dioxide, phase transition, amino acids, ferroelectricity.

## 1. INTRODUCTION

The ferroelectric materials containing amino acids in general and glycine in particular (triglycine sulfate [1 – 4], glycine sodium nitrate [5], glycine silver nitrate [6], glycine phosphate [7], etc.) have been widely applied in biosensors, infrared sensors, NLO, memories [4, 8, 9] due to their good mechanical and electrical stability, wide transparency and high sensitivity. In this context, glycine sodium nitrate (GSN) is known as a semi-organic compound from sodium nitrate and glycine which create hydrogen bonds between donor carboxylic acid (COOH) and accepter amino ($NH_2$) [5], resulting in the formation of valuable electro-optic properties for NLO applications. From our point of view, the current applications of GSN are not commensurate with its potential. Indeed, some primary properties of GSN are even better than those of triglycine sulfate (TGS) such as the considerably high spontaneous polarization $P_s \sim 1$ μC/cm$^2$ with a small coercive field ($E_c \sim 5$ kV/cm) at room temperature, the higher Curie point of $T_c \sim 56$ °C in comparison with 49 °C of TGS [5]. While TGS characteristics have been regularly adjusted to meet new practical requirements by combining with other materials or adopting appropriate substances, GSN has been of little interest. As far as we are concerned, there have been no works dedicated to the improvement of primary GSN properties. GSN is mostly applied in the form of as-grown single crystals. In today's science and technology era, it is rare to use pristine material in practice. In this regard, improving GSN electrophysical properties is necessary to expand not only our fundamental understanding, but also the scope for new applications.

In the present work, nanoparticles of silicon dioxides ($nSiO_2$) were utilized to synthesize a composite with GSN. Silicon dioxide has been found in several applications in the role of a good insulator with high thermal and electrical stability [10 – 13]. Especially, at the nanoscale level, it has large specific surface areas that enhance the interactive ability with other components. In this study, different compositions (weight ratios) of $nSiO_2$ and GSN will be considered to evaluate the influence of $nSiO_2$ on structures as well as the electrophysical properties of GSN.

## 2. SAMPLES SYNTHESIS AND EXPERIMENTAL TECHNIQUES

The procedure for the preparation of $nSiO_2$/GSN nanocomposite is illustrated in Fig. 1 using the slow evaporation technique. Firstly, the two starting materials of glycine and $NaNO_3$ with a mole ratio of 1:1 were dissolved into deionized water to get a saturated solution at room temperature. After 2 h of stirring using a magnetic stir in a closed bottle, nanoparticles of silicon dioxide stored in the form of hydrosol ranged in size of 20 – 200 nm [14] were added so that the mass ratio of $nSiO_2$:(glycine + $NaNO_3$) was of 0.1:1, 0.2:1, 1:1 and 3:1. All substances were mixed by the stirrer for 1h, then the mixture was kept at 20 °C to slowly evaporate for about 40 days. Finally, a fresh mixture was obtained, taken out, dried at 100 °C for 2 h to remove residual water and pressed into circle samples with a radius

* Corresponding author. Tel.: +84868844320.
E-mail address: *maibichdung@iuh.edu.vn* (B. D. Mai)

of 2 mm and a thickness of 1 mm. A silver glue was applied on a large surface to make electrodes for dielectric measurements. For comparison, the crystals of GSN were also synthesized through the same procedure.

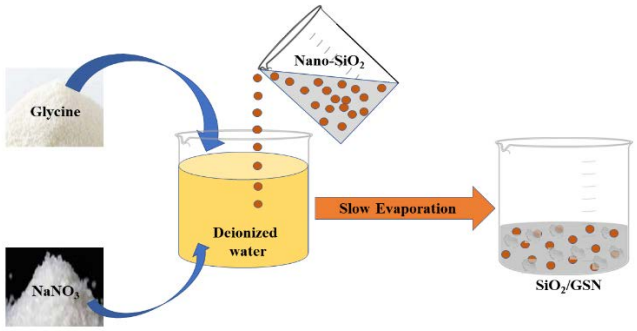


**Fig. 1.** Scheme for preparation of $nSiO_2$/GSN nanocomposite

Before measuring dielectric characteristics, the structures of $nSiO_2$/GSN nanocomposite samples were carefully investigated using X-ray diffraction (Rigaku Ultima IV) and Fourier-transform infrared spectroscopy (Bruker Tensor 37, USA). For testing electrophysical properties, a silver conductive paste (7440-22-4-Sigma-Aldrich) was applied on the sample surfaces. The ferroelectric/ferroelectric phase transition was observed on the spectra of dielectric constant (GW Instek LCR-821 meter) from 30 – 110 °C, while the relaxation features were conducted in the range of $1 - 10^7$ Hz on an impedance gain/phase analyzer (Solartron-1260A, UK). Besides, the switching characteristics of the composite were taken on a Precision LC tester (Radiant Technology, Korea).

## 3. EXPERIMENTAL RESULTS AND DISCUSSION

### 3.1. Structure features

For GSN which is mostly applied in practice in the form of single crystals, the quality of the crystalline structure is one of the most important criteria considered to confirm the success of a preparation process. In our case with the participation of $nSiO_2$, the results could be very different from the pure samples, and therefore the crystalline structure of the synthesized composite must be checked more carefully. According to the exported XRD patterns (Fig. 2), the obtained GSN crystals were reliable with several characteristic peaks at 2θ = 13.97° (-201), 18.18° (110), 19.49° (-111), 22.24° (002), 23.09° (-311), 25.04° (-402), 26.15° (310), 28.31° (400), 31.82° (202), 33.88° (311), 34.42° (-313), 36.49° (220) and 39.56° (-220) which are in good agreement with those reported in literature [5, 15]. It is worth to note that our experiments and reported works [5, 15] showed a high sensitivity of crystalline structure to synthesis conditions. In this regard, there were differences in XRD patterns observed by the authors. In our case, all main peaks of GSN were detected. In the presence of $nSiO_2$ in the structures, the crystallinity degree decreased, even though the positions of peaks were not moved (Fig. 2). For samples with $nSiO_2$:GSN of 0.2:1 or lower $nSiO_2$ content, most of the GSN peaks were found, indicating the formation of the crystalline structure of GSN in the composite. However, at higher than 75 % of $nSiO_2$, the crystalline structure might be not formed with only a few small peaks in the XRD pattern (Fig. 2). Likely, the $nSiO_2$ disturbed the growth of GSN crystals.

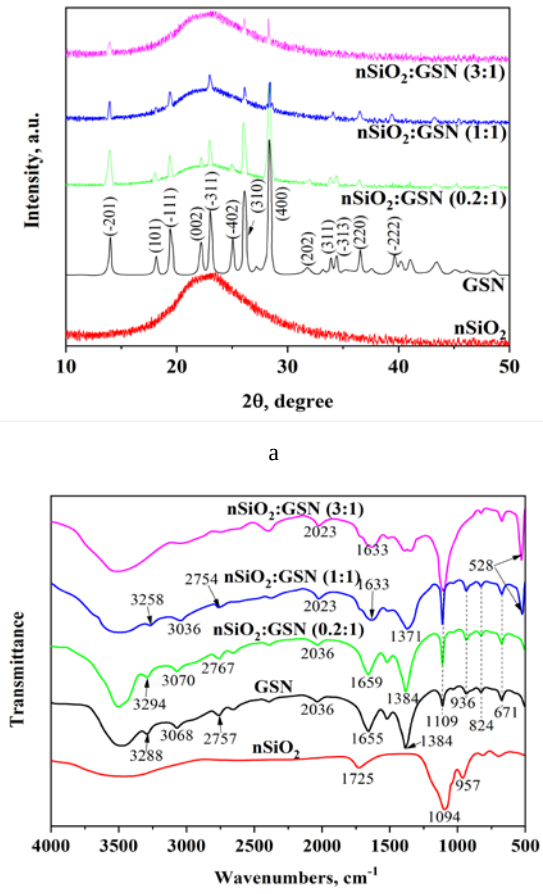


**Fig. 2.** a – XRD patterns; b – FTIR spectra of $nSiO_2$, GSN and the composites at different compositions

To get more information about the structure of GSN and $nSiO_2$/GSN nanocomposite, FTIR spectra have been taken (Fig. 2). Firstly, the reliability of $nSiO_2$ was once again confirmed with the main characteristic adsorption peak of Si-O-Si detected at 1094 $cm^{-1}$ [16]. Besides, the peaks of 957 and 1725 $cm^{-1}$ might be given by OH and Si-OH groups, respectively [17]. The presence of OH was probably related to the residual water in $SiO_2$ [18]. In the absence of $nSiO_2$ (Fig. 2 b), the pure GSN crystals contain typical groups of $NH_3^+$ stretching (3288 $cm^{-1}$), $NH_3^+$ and $COO^-$ zwitterions (3068, 2757 $cm^{-1}$), asymmetrical bending and torsional oscillation of $NH_3$ (2036 $cm^{-1}$) [19], asymmetrical stretching mode of $COO^-$(1655 $cm^{-1}$), asymmetrical stretching of $NO_3^-$ (1384 $cm^{-1}$) [20], $CH_2$ rocking (1109, 936 $cm^{-1}$), $NO_3^-$ vibrations (824 and 671 $cm^{-1}$) [$NO_3$] [19]. Because pure GSN and the $nSiO_2$/GSN composite were prepared via the same procedure, the above observation of characteristic functional groups for GSN insists that the proposed synthesis steps are reliable. Indeed, for samples with $nSiO_2$:GSN = 0.2:1 or lower $nSiO_2$ content, most of the listed peaks for GSN were obtained (Fig. 2 b). However, increasing $nSiO_2$ content led to the appearance of a peak at 528 $cm^{-1}$ when accompanied by the gradual disappearance

of GSN peaks. The wavenumber of 528 $cm^{-1}$ seems to be originated from free glycine [20] that is probably left over after synthesis because of not combining with $NaNO_3$ to form GSN. This is in good agreement with the decreased crystallinity observed in XRD patterns toward high-$nSiO_2$-content samples.

### 3.2. Phase transition

Phase transition plays a leading role in most the applications in electronics using ferroelectric-based materials. In our experiments, the phase transition for the composite was investigated by measuring the dependences of dielectric constant $\varepsilon$ on temperature $T$ from 30 to 100 °C (Fig. 3). Observing that $\varepsilon(T)$ has peaks at 60.2, 63.8 and 69.2 °C for samples of $nSiO_2$:GSN = 0.2:1, 1:1 and 3:1, respectively. In other words, in the presence of $nSiO_2$, the phase transition temperature was higher than that of pure GSN ($T_c$ = 56 °C [5]). Besides, the higher the $nSiO_2$ content was, the greater the phase transition temperature obtained (Fig. 3). This was good because the ferroelectric phase was expanded. However, for the composite samples with high $nSiO_2$ content, the values of dielectric constant sharply dropped (< 40) when $nSiO_2$ content was higher than 50 % as seen in the inset of Fig. 3. According to our experiments, the highest $\varepsilon$ might reach 1000 at $nSiO_2$:GSN = 0.2:1 and this composition can be considered optimal. The explanation for that will be given in detail in this paper.

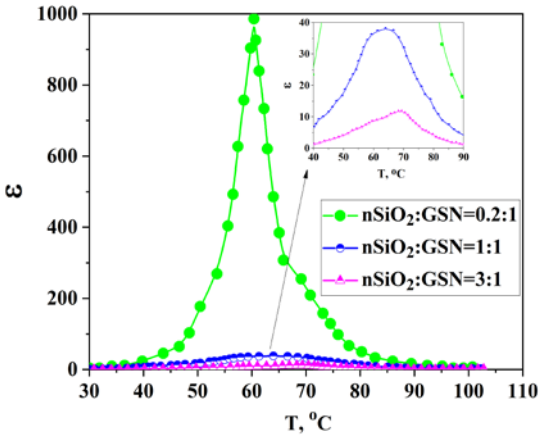


**Fig. 3.** The results for phase transition testing for composite samples containing different $nSiO_2$ content

### 3.3. Switching properties

Switching properties characterizing the reversal of polarized molecules, groups of molecules or domains are very important when applying ferroelectrics in practice. Besides, clarifying their switching properties may help to figure out the behaviors of structural elements in materials [21]. The above structural analysis (XRD, FTIR) and phase transition indicated that the composite samples with the increased $nSiO_2$ content were of lower quality. To confirm once again this conclusion, the switching features for the synthesized composite were also investigated as presented in Fig. 4. Firstly, it is worth to emphasize that the dielectric hysteresis loop for pure crystals of GSN obtained in our preparation process has a similar shape to that reported in the literature [5]. Besides, the values of saturated polarization ($P_s$ = 0.96 μC/$cm^2$), remnant polarization ($P_r$ = 0.83 μC/$cm^2$) and coercive field ($E_c$ = 3.28 kV/cm) at room temperature (Table 1) were comparable with the published data [5]. When combined with $nSiO_2$, the decrease in $P_s$, $P_r$ and the increase in $E_c$ were detected (Table 1). The P-E loops gradually lost the characteristic shape with increasing $nSiO_2$ content (Fig. 4). This anomaly seems to be consistent with those of XRD, FTIR and $\varepsilon(T)$ described above. According to our experiments, samples with the weight ratio of $nSiO_2$:GSN = 0.2:1 can be considered as optimal because any deviation from that led to unexpected consequences. Indeed, the higher $nSiO_2$ content might reduce the dielectric constant (Fig. 3) and hinder the switching process (Fig. 4), while the lower $nSiO_2$ content resulted in the reduction of phase transition temperature (Fig. 3).

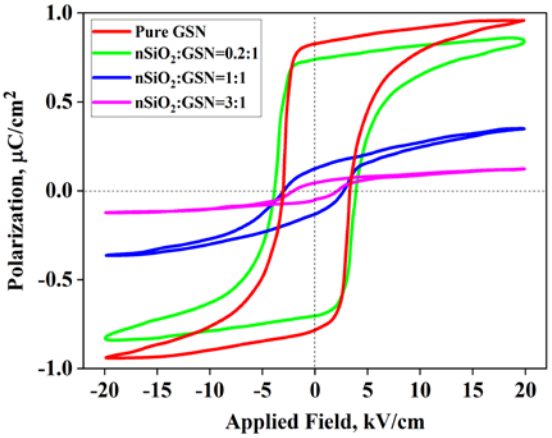


**Fig. 4.** P-E hysteresis loops for pure GSN and composite samples with different compositions at room temperature and 1 kHz

**Table 1.** The values of $P_s$, $P_r$, $E_c$ for the composite at different compositions

| Composite samples | $P_s$, μC/$cm^2$ | $P_r$, μC/$cm^2$ | $E_c$, kV/cm |
|---|---|---|---|
| Pure GSN | 0.96 | 0.83 | 3.28 |
| $nSiO_2$:GSN = 0.2:1 | 0.86 | 0.73 | 3.94 |
| $nSiO_2$:GSN = 1:1 | 0.35 | 0.13 | 2.69 |
| $nSiO_2$:GSN = 3:1 | 0.12 | 0.05 | 2.07 |

### 3.4. Frequency response of $nSiO_2$/GSN composite

Because the frequency is related to the reversal speed of the external electric field that directly affects the behavior of charged groups in materials, analyzing electrophysical parameters at different frequencies is valuable to explore the structure as well as ferroelectricity of ferroelectric-based compounds. The samples of optimal $nSiO_2$:GSN = 0.2:1 were chosen for these experiments. The results are shown in Fig. 5 in the form of frequency dependences of the real $\varepsilon'$ (Fig. 5 a) and the imaginary $\varepsilon''$ (Fig. 5 b) permittivity at different temperatures in the polar phase ($T < T_c$ = 60.2 °C). Obviously, at each temperature, the increase in frequency led to the monotonic decrease in $\varepsilon'$ (Fig. 5 a) that is in good agreement with those of pure GSN crystals [5]. However, in the dependences of $\varepsilon''(f)$ (Fig. 5 b), a deviation from the reported pure GSN was found with the appearance of a peak. Noted [22] that the presence of peaks on $\varepsilon''(f)$ at frequencies of $10-10^7$ Hz was also observed in TGS which belongs to

the glycine-containing ferroelectric family as GSN. This peak shifted toward higher frequencies at higher temperatures (Fig. 5 b), indicating the activation nature of the relaxation process. The relaxation time $\tau$ can be calculated from the relaxation frequencies $f_r$ taken at the peaks by $\tau=1/2\pi f_r$.

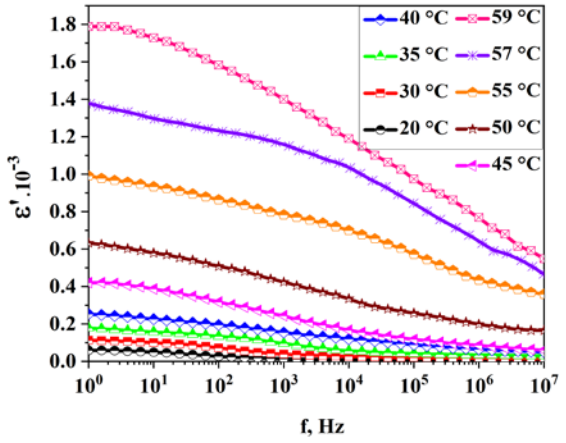


a

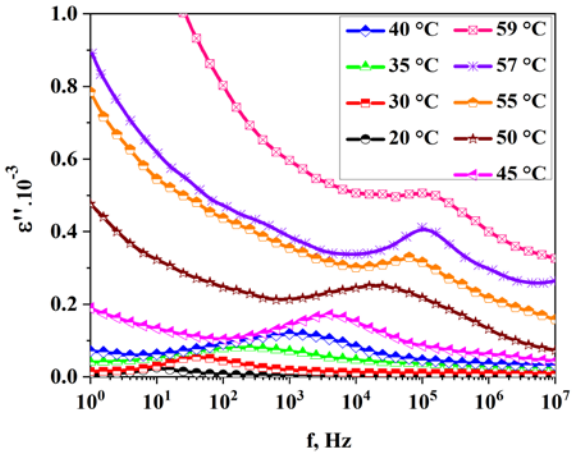


b

**Fig. 5.** Frequency dependences of dielectric permittivity at different temperatures under phase transition point for the composite samples of $nSiO_2$:GSN = 0.2:1: a – real parts; b – imaginary parts

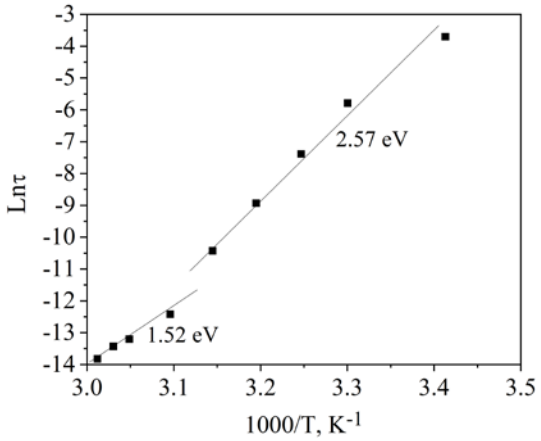


**Fig. 6.** Inverse temperature dependences of relaxation time at different temperatures under phase transition point for the composite samples of $nSiO_2$:GSN = 0.2:1

The dependences of relaxation time on inverse temperature are presented in Fig. 6. Apparently, there were two relaxation processes corresponding to two activation energies of 1.52 and 2.57 eV observed at $10 – 10^7$ Hz in the ferroelectric phase of $nSiO_2$/GSN.

### 3.5. Discussion

Firstly, the obtained results allow us to conclude that the use of $nSiO_2$ content higher than the weight ratio of 0.2:1 or 16.7 wt.% may cause several consequences as the drop of $\varepsilon$ (Fig. 3) and $P_s$ (Fig. 4), as well as the distortion of the dielectric P-E hysteresis (Fig. 4). The reason for that might be related to the presence of $nSiO_2$ that hindered the contact between glycine and $NaNO_3$ during the growth of crystals evidenced by the lack of peaks in the XRD pattern (Fig. 2 a) and the rise of free glycine left over in FTIR spectra (Fig. 2 b), resulting to the shrinking of GSN volume in the synthesized samples. Consequently, the ferroelectricity of the composite showed less clearly. Notably, regardless of whether the free glycine is left over or not, the addition of the dielectric component of $nSiO_2$ indisputably reduces the GSN volume and therefore the ferroelectricity becomes weaker. Commonly, the change of electrophysical parameters gradually occurs during heating in the polar phase [1, 2]. Likely, the main reason in our case was not associated with that due to the sudden drop of $\varepsilon$ and $P_s$.

When increasing $nSiO_2$ content, the observed increase in phase transition temperature $T_c$ (Fig. 2) and coercive field $E_c$ (Fig. 3) might be referred to the stronger interaction between $nSiO_2$ nanoparticles and GSN crystals through hydrogen bonds due to residual water. Indeed, the residual water molecules can be completely removed from $nSiO_2$ at higher than 500 °C [18], while the synthesized samples were heated up to 100 °C. If this assumption was true, the polar phase of GSN became more stable and turned into the paraelectric phase at higher temperatures. At the same time, the greater number of $nSiO_2$ nanoparticles surrounding GSN crystals could create a stronger interaction, leading to the difficulty in moving domain walls i.e. to the rise of $E_c$.

The appearance of maxima in $\varepsilon''(f)$ can be understood because the interaction between $nSiO_2$ nanoparticles and GSN crystals could cause the increase in viscosity for that the relaxation frequencies $f_m$ can be estimated as follows [1]:

$$f_m = \frac{1}{\eta D}, \quad (1)$$

where $\eta$ is the viscosity coefficient and $D$ is the width of domains. With increasing temperature, the viscosity decreased, leading to an increase in relaxation frequencies (Fig. 5 b).

The activation energies of 1.52 and 2.57 eV are significantly higher than those reported in the literature for pure GSN [5]. Known [5, 23] that the activation energy of proton transfer in glycine zwitterion as for GSN is about 0.69 eV. It allows us to assume that there was the contribution of hydrogen bonds to potential barriers. In this regard, the decrease in $E_a$ from 2.57 to 1.52 eV might be referred to less stable hydrogen bonds with increasing temperature.

## 4. CONCLUSIONS

The study successfully estimated the optimal content of silicon dioxide nanoparticles for preparation of composite with glycine sodium nitrate as 16.7 wt.% at which the phase transition point increased by 4.2 °°C while the dielectric constant and spontaneous polarization slightly decreased. The higher $nSiO_2$ content might inhibit the growth of GSN crystals, resulting in a sharp decrease in dielectric constant and spontaneous polarization, as well as the distortion of dielectric hysteresis loops. Besides, the increased $nSiO_2$ may strengthen the interaction between $nSiO_2$ and GSN, and therefore drag the phase transition point toward higher temperatures. The obtained results provide a considerably simple but effective approach for improving the properties of the amino-acid based ferroelectric family.

**REFERENCES**


1. **Mai, B. D.** Analyzing Frequency Spectra of Dielectric Loss to Clarify Influence of L,α-alanine Doping on Phase Transition in Triglycine Sulfate *Materials Science - Medziagotyra* 28 (2) 2022: pp. 151 – 156. https://doi.org/10.5755/j02.ms.29313
2. **Nguyen, H.T.** Anomalous P-E Hysteresis Loops of Ferroelectric Nanocomposites Containing Nanocellulose and Hydrogen – Bonded Ferroelectric of Triglycine Sulfate Under Influence of Composition, Temperature and Moisture *Materials Science - Medziagotyra* Early Access 2022. https://doi.org/10.5755/j02.ms.30250
3. **Ghane-Motlagh, R., Fammels, J., Danilewsky, A.N., Pelz, U., Woias, P.** Effect of Surfactants on The Growth and Characterization of Triglycine Sulfate Crystals *Journal of Crystal Growth* 563 2021: pp. 126081 (1 – 5). https://doi.org/10.1016/j.jcrysgro.2021.126081
4. **Munje, R.D., Muthukumar, S., Jagannath, B., Prasad, S.** A New Paradigm in Sweat Based Wearable Diagnostics Biosensors Using Room Temperature Ionic Liquids (RTILs) *Scientific Reports* 7 (1950) 2017: pp. 1 – 12. https://doi.org/10.1038/s41598-017-02133-0
5. **Tyagi, N., Sinha, N., Kumar, B.** Evidence of Sustained Ferroelectricity in Glycine Sodium Nitrate Single Crystal *Current Applied Physics* 14 (2) 2014: pp. 156 – 160. https://doi.org/10.1016/j.cap.2013.11.005
6. **Choudhury, R.R., Panicker, L., Chitra, R., Sakuntala, T.** Structural Phase Transition in Ferroelectric Glycine Silver Nitrate *Solid State Communications* 145 (7 – 8) 2008: pp. 407 – 412. https://doi.org/10.1016/j.ssc.2007.11.010
7. **Dacko, S., Czapla, Z., Baran, J., Drozd, M.** Ferroelectricity in $Gly{\cdot}H_3PO_3$ Crystal *Physics Letters A* 223 (3) 1996: pp. 217 – 220. https://doi.org/10.1016/S0375-9601(96)00698-6
8. **Manjunatha, J.G.G.** A Novel Poly (Glycine) Biosensor Towards the Detection of Indigo Carmine: A Voltammetric Study *Journal of Food and Drug Analysis* 26 (1) 2018: pp. 292 – 299. https://doi.org/10.1016/j.jfda.2017.05.002
9. **Deshpande, M.P., Gujarati, V.P., Patel, K.N., Chaki, S.H.** A Study on Thermal and Optical Properties of Glycine Sodium Nitrate Crystals *Advanced Materials Letters* 8 (2) 2017: pp. 170 – 173. https://doi.org/10.5185/amlett.2017.6887
10. **Miyata, Y., Nakamukai, Y., Azevedo, C.T., Tsuchida, A., Morita, M., Oshikane, Y., Uchikoshi, J., Kawai, K., Arima, K., Morita, M.** Electroluminescence in Metal-Oxide-Semiconductor Tunnel Diodes with a Crystalline Silicon/Silicon Dioxide Quantum Well *Micro and Nanostructures* 2022: pp. 207228 (in press). https://doi.org/10.1016/j.micrna.2022.207228
11. **Abu-Hamdeh, N.H. Alazwari, M.A. Salilih, E.M., Mohammad Sajadi, S., Karimipour, A.** Improve the Efficiency and Heat Transfer Rate' Trend Prediction of a Flat-Plate Solar Collector Via a Solar Energy Installation by Examine the Titanium Dioxide/Silicon Dioxide-Water Nanofluid *Sustainable Energy Technologies and Assessments* 48 2021: pp. 101623. https://doi.org/10.1016/j.seta.2021.101623
12. **Avotina, L., Pajuste, E., Romanova, M., Enichek, G., Zaslavskis, A., Kinerte, V., Avotins, J., Dehtjars, Y., Kizane, G.** Surface Morphology of Single and Multi-Layer Silicon Nitride Dielectric Nano-Coatings on Silicon Dioxide and Polycrystalline Silicon *Materials Science – Medziagotyra* 26 (1) 2020: pp. 25 – 29. https://doi.org/10.5755/j01.ms.26.1.21479
13. **Grigaliūnas, V., Abakevičienė, B., Grybas, I., Gudonytė, A., Kopustinskas, V., Viržonis, D., Naujokaitis, R., Tamulevičius, S.** Two-step Fabrication of Large Area $SiO_2$/Si Membranes *Materials Science – Medziagotyra* 18 (4) 2012: pp. 325 – 329. https://doi.org/10.5755/j01.ms.18.4.3090
14. **Mai, B.D., Nguyen, H.T., Hoang, D.Q.** A Novel Composite from Nanodispersed Silica and an Organic Ferroelectric of Diisopropylammonium Bromide: Preparation, Characterization and Dielectric Properties *Materials Transactions* 60 (10) 2019: pp. 2132 – 2136. https://doi.org/10.2320/matertrans.MT-M2019157
15. **Sankar, R., Ragahvan, C.M., Mohan Kumar, R., Jayavel, R.** Growth and Characterization of Bis-Glycine Sodium Nitrate (BGSN), a Novel Semi-Organic Nonlinear Optical Crystal *Journal of Crystal Growth* 309 (1) 2007: pp. 30 – 36. https://doi.org/10.1016/j.jcrysgro.2007.08.013
16. **Dubey, R.S., Rajesh, Y.B.R.D., More, M.A.** Synthesis and Characterization of $SiO_2$ Nanoparticles via Sol-gel Method for Industrial Applications *Materials Today: Proceedings* 2 (4 – 5) 2015: pp. 3575 – 3579. https://doi.org/10.1016/j.matpr.2015.07.098
17. **Lu, Y.K., Yan, X.P.** An Imprinted Organic−Inorganic Hybrid Sorbent for Selective Separation of Cadmium from Aqueous Solution *Analytical Chemistry* 76 (2) 2004: pp. 453 – 457. https://doi.org/10.1021/ac0347718
18. **Mai Phuong, N., Neishi, K., Sutou, Y., Koike, J.** Effects of Adsorbed Moisture in $SiO_2$ Substrates on the Formation of a Mn Oxide Layer by Chemical Vapor Deposition *The Journal of Physical Chemistry C* 115 (34) 2011: pp. 16731 – 16736. https://doi.org/10.1021/jp201299w
19. **Besky Job, C., Shabu, R., Anne, R., Paul Raj, S.** Growth and Characterization of Glycine Sodium Nitrate Non-Linear Optical Crystal *Rasayan Journal of Chemistry* 8 (3) 2015: pp. 310 – 315.
20. **Nichol, G.S., Hernandez Paredes, J., Esparza Poncce, H.E., Pacheco Beltran, M., Alvarez Ramos, M.E., Duarte-Moller, A.** Low Temperature Redetermination of The Glycine Sodium Nitrate Structure by Using X-Ray Single Crystal Diffraction Technique *Revista Mexicana De F´Isica S* 54 (1) 2008: pp. 13 – 16.

21. **Artemev, A.** Domain Structures and Switching Properties in Ferroelectric Nanocomposites *Applied Physics Letters* 103 (13) 2013: pp. 132912 (1 – 4). https://doi.org/10.1063/1.4823553

22. **Nguyen, H.T., Sidorkin, A.S., Milovidova, S.D., Rogazinskaya, O.V.** Investigation of Dielectric Relaxation in Ferroelectric Composite Nanocrystalline Cellulose – Triglycine Sulfate *Ferroelectrics* 498 (1) 2016: pp. 27 – 35. https://doi.org/10.1080/00150193.2016.1166835

23. **Gwon, O.Y., Kim, S.Y., No, G.T.** Determination of the Proton Transfer Energies of Glycine and Alanine and the Influence of Water Molecules *Bulletin of the Korean Chemical Society* 16 (5) 1995: pp. 410 – 416. https://doi.org/10.5012/bkcs.1995.16.5.410